

# A Look into the Properties of Carbon Nanotubes

## 0) What are carbon nanotubes?

In the realm of nanotechnology, nanomaterials have multiple applications, ranging from advanced electronics to novel biomedical devices. Nanomaterials are materials whose size are at the scale of nanometers, and one of the most notable of these are carbon nanotubes.

Discovered in the early 1990's, carbon nanotubes have garnered much attention due to their properties. In particular, they exhibit remarkable mechanical strength, electrical & thermal conductivity, and chemical stability. Carbon nanotubes are rolled up sheets of graphene, and there are 2 main types of carbon nanotubes: single- and multi- walled carbon nanotubes (SWCNTs & MWCNTs). In this paper, we can start with more basic structures to delve into the properties of CNTs. SWCNTs are a good place to start, fashioning a more simple structure with their one-atom-thick walls and cylindrical shape. In this paper we will understand the special properties of CNTs through discussing the features of the lattice of graphene, the CNT's physical size and shape, its energy bands, and covalent  $sp^2$  bonds. This will all be divided into sections, each including an ending paragraph relating the content of the section to specific CNT properties and it will become clear as to why CNTs are of great interest.

## 1) Geometry of the Graphene Lattice and Rolling into a SWCNT

By looking at the geometry and shape of Graphene in both its flat and rolled forms, we can start understanding the foundation with which we will work in unpacking some intrinsic characteristics of carbon nanotubes. In its flat form, graphene has a hexagonal lattice structure. Each carbon atom in the structure bonds covalently to 3 other carbon atoms in  $sp^2$  hybridized bonds, forming 120 degree angles between each bond and creating a planar, honeycomb-like structure. The unit cell of graphene has

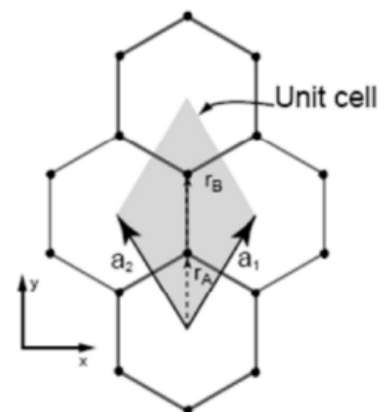


**Figure 1:** Primitive unit cell and primitive lattice vectors  $a_1$ ,  $a_2$

primitive lattice vectors  $a_1 = \frac{a}{2}\hat{x} + \frac{\sqrt{3}a}{2}\hat{y}$  and  $a_2 = \frac{a}{2}\hat{x} - \frac{\sqrt{3}a}{2}\hat{y}$ , with 2 carbon atoms in each unit cell.

In looking at graphite in its “rolled” form, we can consider chirality and diameter of the SWCNT cylinder. Chirality is an important concept to become familiar with and defines 3 different families of SWCNTs. Chirality

can be understood by measuring a chiral angle, the angle between the PLV  $a_1$  of the unit cell and the chiral vector  $C_h = na_1 + ma_2$ , across which

the graphene is folded over into a cylinder. The 3 classifications of SWCNTs are based on chirality measurements  $(n, m)$  and are called armchair ( $n = m$ ), zig-zag ( $n, 0$ ), and chiral ( $n \neq m$ ) nanotubes. Aside from chirality, the cylinder has a

circumference of  $|C_h| = \pi d$  with  $d$  being the diameter of the cylinder. SWCNTs can have diameters between 0.4nm-4.5nm and can have lengths ranging between the scale of nanometers and the scale of centimeters [1].

It will be shown that the indices  $(n, m)$  of a SWCNT will control the features of its energy bands, impacting the electronic properties of the material. This means that different chiralities and diameters will determine if a CNT acts as a conductor, or a semiconductor. The length of the CNT impacts other properties, such as electrical conductivity, Young's modulus, and shear modulus which all grow along with the length of a nanotube.

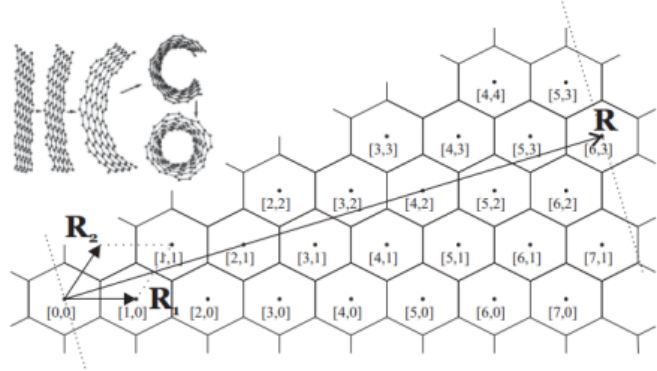


**Figure 2:** Shows indices  $(n, m)$ , with the longest vector being the chiral vector and  $R_1, R_2$  being vectors of the unit cell. notice diameter becomes larger as values for  $(n, m)$  grow.

## 2) Schrodinger Equation and Energy Bands

The energy band structure of a SWCNT can tell us a few things about how it will behave as a nanomaterial through its electronic properties. To be able to examine the traits of the energy bands and analyze them, it will be essential to calculate the dispersion relation by solving the Schrodinger equation. This can be done using a variety of different approaches and not all methods yield the same exact results. However, one thing the results should always agree on is that general features of the energy bands should remain similar and lead to the same conclusions.

It won't be very useful within the scope of this paper to meticulously explain the process of solving this problem; but rather we can go through a general overview of how the

dispersion relations are obtained. The flow can be followed using the equations [2] in Figure

3. As a note,  $(N_x, N_y) = (n, m)$ .

To understand the electronic properties of carbon nanotubes (CNTs), we can reasonably start with graphene, applying periodic boundary conditions to reflect the tubular structure of CNTs. This begins with a Bloch function representing an electron's wavefunction in graphene's unit cell (eq. 1).

Utilizing the Linear

Combination of Atomic Orbitals (LCAO) approach, we consider graphene's two carbon atoms per cell, and express the desired eigenfunction (eq. 2) as a linear combination of

$$E_q(k) = \pm \gamma_0 \left[ 1 \pm 4 \cos \left( \frac{q\pi}{N_x} - \frac{N_y ka}{2} \right) \cos \left( \frac{ka}{2} \right) + 4 \cos^2 \left( \frac{ka}{2} \right) \right]^{1/2} \quad (-\pi < ka < \pi) \quad (q = 1, \dots, N_x).$$

for a chiral SWCNT (12)

$$E_q^a(k) = \pm \gamma_0 \left[ 1 \pm 4 \cos \left( \frac{q\pi}{N_x} \right) \cos \left( \frac{ka}{2} \right) + 4 \cos^2 \left( \frac{ka}{2} \right) \right]^{1/2} \quad (-\pi < ka < \pi) \quad (q = 1, \dots, N_x),$$

for an armchair SWCNT (13)

$$E_q^z(k) = \pm \gamma_0 \left[ 1 \pm 4 \cos \left( \frac{\sqrt{3}ka}{2} \right) \cos \left( \frac{q\pi}{N_y} \right) + 4 \cos^2 \left( \frac{q\pi}{N_y} \right) \right]^{1/2} \quad \left( -\frac{\pi}{\sqrt{3}} < ka < \frac{\pi}{\sqrt{3}} \right) \quad (q = 1, \dots, N_y).$$

for a zig-zag SWCNT (14)

implementation while preserving general energy band properties. Equations 12, 13, and 14 [3] present similar results for armchair, zig-zag, and chiral nanotubes, using a  $g(k)$ -esque variable.

By using these energy values, you can see the structure of the bands. In Figure 4, we plot a few bands across the 1<sup>st</sup> Brillouin zone of the hexagonal Wigner-Seitz unit cell constructed from a point in the center of the primitive unit cell from Figure 1. The energy

Bloch Functions	Schrodinger Equation
$\Phi_j(\vec{k}, \vec{r}) = \frac{1}{\sqrt{N}} \sum_{\vec{R} \in G} e^{i\vec{k} \cdot \vec{R}} \phi_j(\vec{r} - \vec{R}) \quad (1)$ $\Psi_a(\vec{k}, \vec{r}) = \sum_{j=1}^2 C_{aj}(\vec{k}) \Phi_j(\vec{k}, \vec{r}) \quad (2)$	$\det[\mathbf{H} - E_i \mathbf{S}] = 0 \quad (3)$ $H_{jj'}(\vec{k}) = \langle \Phi_j   \mathbf{H}   \Phi_{j'} \rangle \quad (4)$ $S_{jj'}(\vec{k}) = \langle \Phi_j   \Phi_{j'} \rangle \quad (5)$
Matrix Elements	Schrodinger Equation w/ Values & Dispersion Relation
$\langle \Phi_A   \mathbf{H}   \Phi_A \rangle \approx 2\varepsilon_{2p} \quad (6)$ $\mathbf{H}_{AB} = \mathbf{H}_{AB}^* = \gamma_1 (1 + e^{i\vec{k} \cdot \vec{a}} + e^{-i\vec{k} \cdot \vec{a}}) = \gamma_1 g(\vec{k}) \quad (7)$ $S_{AB} = S_{AB}^* = \gamma_0 g(\vec{k}) \quad (8)$ $S_{AA} = S_{BB} = 1 \quad (9)$	$\det \begin{bmatrix} \varepsilon_{2p} - E_i & (\gamma_1 - \gamma_0 E_i) g(\vec{k}) \\ (\gamma_1 - \gamma_0 E_i) g^*(\vec{k}) & \varepsilon_{2p} - E_i \end{bmatrix} = 0 \quad (10)$ $E_i(\vec{k}) = \frac{\varepsilon_{2p} \pm  g(\vec{k})  \gamma_1}{1 \pm  g(\vec{k})  \gamma_0} \quad (11)$

**Figure 3:** Includes equations numbered 1-11, This table shows the flow of how the dispersion relation is found.

Bloch functions for each participating electron. By solving the Schrödinger equation, we arrive at equation 3, deriving values for H and S (eqs. 6,7,8 & 9) using the tight-binding approximation and by doing some calculations. This leads to the dispersion relation in equation 11, employing an energy vector  $g(k)$  for band visualization, simplifying

bands show that all armchair SWCNTs act as metals since you can see that they overlap at the fermi energy (calculated to be  $\varepsilon_F = 0$  for SWCNTs). For non-armchair nanotubes,  $\frac{1}{3}$  act as metals, and the other  $\frac{2}{3}$  act as semimetals, which can again be confirmed if we look at more  $(n, m)$  values. Another feature in these graphs for non-armchair nanotubes is that at smaller diameters the nanotubes act more as narrow-gap semiconductors than those with larger diameters. This can be seen as you go down the zig-zag & chiral columns in Figure 4. It can also be noted that chiral nanotubes have asymmetrical energy bands due to the nature of the chirality here where  $(n \neq m)$ , illuminating yet another way in which the flow of electricity through the lattice can be modified.

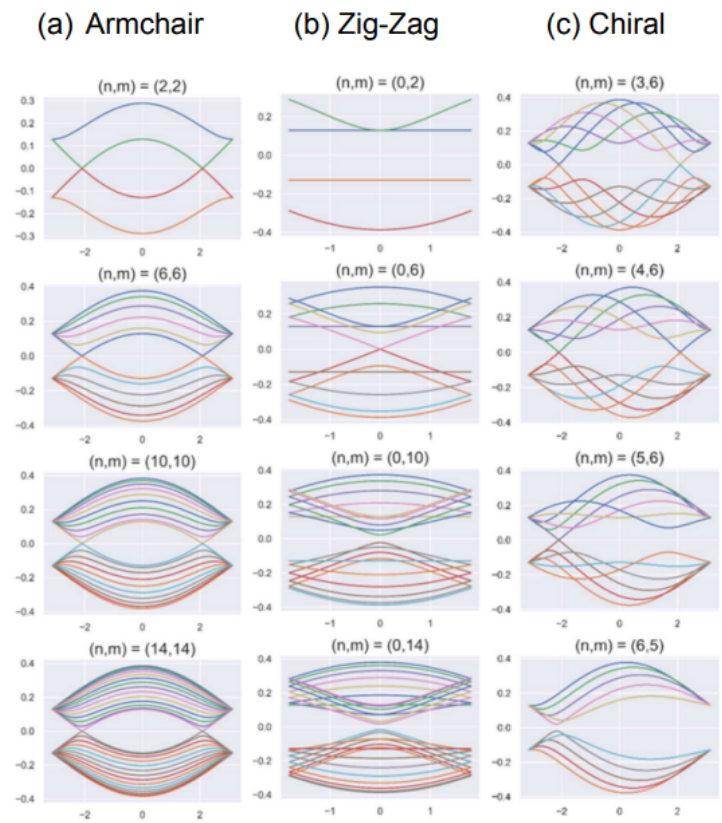


**Figure 4:** Energy band structures for different values of  $(n, m)$ . Each column (a), (b), (c) corresponds to a type of nanotube and is labeled as such.

### 3) Binding Forces & Structure of the SWCNT

The binding forces and distinctive structural features of single-walled carbon nanotubes (SWCNTs), particularly their nanoscale dimensions, play a crucial role in shaping their mechanical, electrical, and thermal properties. As established in the first section, SWCNTs are characterized by a hexagonal lattice of carbon atoms, each bonded to three others via strong  $sp^2$  hybridized covalent bonds. This arrangement not only creates a planar bond geometry but also contributes significantly to the bonds' strength. The one-dimensional nature and high aspect ratio of SWCNTs

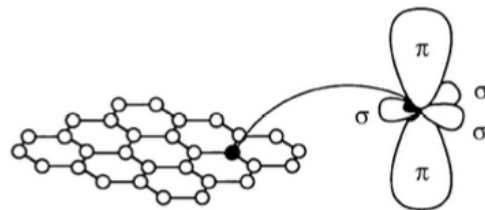


**Figure 5:**  $sp^2$  hybridized orbital in graphene. notice the directions of the pi-orbitals: perpendicular to the material.

further define their physical characteristics, underpinning the exceptional properties for which SWCNTs are renowned.

The  $sp^2$  bonding and one-dimensional structure of SWCNTs affect their electronic properties. The delocalized  $\pi$ -electrons (Figure 5 [4]) arising from the  $sp^2$  bonds allow the electrons to move adjacent to the surface of the graphene, and contribute to the formation of distinct electronic energy bands. These bands are crucial in determining whether an SWCNT behaves as a metal or a semiconductor, a distinction that hinges on the nanotube's chirality and diameter. This electronic structure enables SWCNTs to exhibit high electrical conductivity, especially in armchair configurations as we saw in the last section. Electrical conductivity can also be modified by controlling the length of the nanotube (Figure 6 [5]).

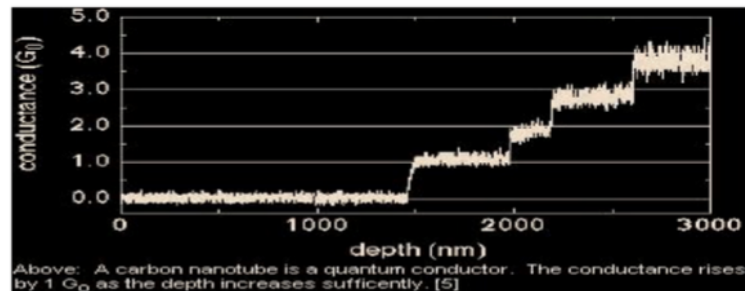


**Figure 6:** Electrical conductance increases with depth of CNT

The thermal properties of SWCNTs can too be explored here, and are intimately linked again to their bonds, lattice structure and geometric aspects. SWCNTs are known to have high thermal conductivity which can be attributed to the efficient lattice vibrational waves, or phonons, facilitated by the strong  $sp^2$  bonds. The seamless and defect-free alignment of these bonds allows phonons to propagate with minimal scattering, enhancing the nanotubes' ability to conduct heat. This effect is augmented in considering the

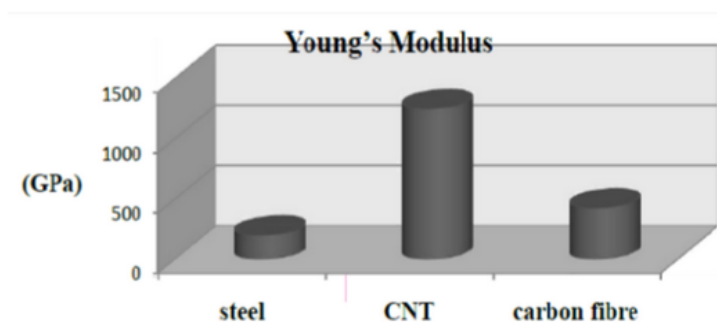


**Figure 7:** Young's modulus of the CNT in comparison to other materials known for their strength.

one-dimensional nature of SWCNTs, which restricts phonon scattering in lateral directions, and increases the efficiency of phonon transportation down its singular dimension, further boosting their thermal conductance.

SWCNTs' mechanical strength is largely a function of their  $sp^2$  hybridized bonds and structural configuration and can be encapsulated by their high Young's and shear moduli which measure elasticity of the material. These measures increase with the length of the CNT. The strong  $sp^2$  covalent bonds work in great synergy with the nano-cylindrical shape of SWCNTs in fortifying the

entire structure. The robustness of these covalent bonds imparts exceptional tensile strength (Figure 7 [5]), while the hexagonal lattice arrangement offers resistance to deformation. The high aspect ratio of SWCNTs also contributes to their resilience, allowing them to withstand significant stress and strain without failure. The cylindrical shape of CNTs extends this structural fortification when regarding effects on the quantum scale from the free or mostly-free electrons (from the  $\pi$ -bonds) in helping maintain a stable shape with their electric forces.

#### **4) Discussion**

The versatile and strongly defined properties of carbon nanotubes make them useful for many things. Their formidable strength, efficient heat conductance, high electrical conductivity, and the ability to mindfully engineer these metrics make CNTs ideal for applications in a wide range of fields, from advanced material science to cutting-edge electronics and energy technologies. In the realm of aerospace and automotive industries, their lightweight yet strong composition is pivotal in developing more efficient, durable materials. In the electronics sector, their unique electrical properties are being harnessed for next-generation electronic devices, including flexible displays and high-capacity batteries. The ability of carbon nanotubes to efficiently dissipate heat also positions them as crucial components in thermal management solutions for high-performance computing systems. This multifaceted utility underscores why carbon nanotubes continue to attract significant research and development focus, heralding a new era of material innovation.

#### **References**

- [1] Monthioux, M., Serp, P., Flahaut, E., Razafinimanana, M., Laurent, C., Peigney, A., & Broto, J. M. (2010). Introduction to carbon nanotubes. Springer handbook of nanotechnology, 47-118.
- [2] Aziz N Mina et al. 2012. Simulation of the Band Structure of Graphene and Carbon Nanotube. Journal of Physics. Conf. Ser. 343 012076
- [3] Gisbertz K.J.H. 2012. Dispersion relations of carbon nanotubes
- [4] Jorio, A. & Saito, R. & Dresselhaus, G. & Dresselhaus, M.S.. (2011). The sp<sup>2</sup> Nanocarbons: Prototypes for Nanoscience and Nanotechnology. Raman Spectroscopy in Graphene Related Systems. 1-15.
- [5] Attar, S., & Ranveer, A. (2015). Carbon nanotubes and its environmental applications. J. Environ. Sci. Comput. Sci. Eng. Technol, 4, 304-311.